Gondwana Research, V. 7, No. 4, pp. 1197-1208.

ISSN: 1342-937X

GR Gondwana Research

Provenance and Evolution of the Guarguaráz Complex, Cordillera Frontal, Argentina

Vanina L. López and Daniel A. Gregori*

Cátedra de Geología Argentina, Universidad Nacional del Sur-CONICET, Bahia Blanca, Postal code-8000, Argentina

** Corresponding author: E-mail: usgregor@criba.edu.ar*

(Manuscript received June 18, 2003; accepted April 22, 2004)

Abstract

The Guarguaráz Complex, basement of the Cordillera Frontal, included in the proposed Chilenia Terrane, consists of metasedimentary rocks deposited in clastic and carbonatic platforms. Turbiditic sequences point out to slope or external platform environments. According to geochemical data, the sedimentary protoliths derived through erosion of a mature cratonic continental basement. Volcanic and subvolcanic rocks with N and E-MORB signature were interbeded in the metasedimentary rocks during basin development. A compressional stage, starting with progressive deformation and metamorphism, followed this extensional stage. Continuing deformation led to the emplacement of slices of oceanic crust, conforming an accretionary prism during Late Devonian. The Guarguaráz Complex and equivalent units in western Precordillera and also in the Chilean Coastal Cordillera share common evolutional stages, widely represented along the western Gondwana margin. These evidences imply that Chilenia is not an allochthonous terrane to Gondwana, but a portion of its Early Paleozoic margin. Regional configuration indicates that the Guarguaráz Complex and equivalent units represent the accretionary prism of the Famatinian arc (Middle Ordovician-Late Devonian).

Key words: Provenance, Guarguaráz Complex, Cordillera Frontal, Famatinian arc, Argentina.

Introduction

Neoproterozoic to Lower Paleozoic rocks crop out in western Argentina, along the Puna, Precordillera, Famatina and Cordillera Frontal. The Cordillera Frontal exhibits a Neoproterozoic? - Early Paleozoic basement, covered by Late Paleozoic sequences, whereas Precordillera is constituted by Paleozoic sedimentary rocks (Fig. 1). The Precordillera Cambrian-Ordovician sequences are considered part of the Precordillera terrane (Ramos et al., 1984, 1986), which together with the Northwestern Sierras Pampeanas constitutes the Cuyania terrane (Ramos et al., 1996). The Cuyania terrane accreted to western Gondwana in Late Ordovician times. The Cordillera Frontal basement, assigned to the Chilenia terrane by Ramos et al. (1984), docked to western Gondwana during Late Devonian.

In western Precordillera and Cordillera Frontal crop out mafic-ultramafic belts, assigned by Haller and Ramos (1984) to the Famatinian Ophiolites, and considered as a suture zone between Precordillera and Chilenia terranes (Ramos et al., 1984). Juxtaposition of both terranes was proposed as a west-dipping subduction (Astini et al., 1995, Davis et al., 1999) or east-dipping subduction (Ramos et al., 1984, 1986).

In particular, the configuration of the Chilenia terrane, and time of accretion to Gondwana are matter of debate. Questions about the nature of the protoliths, their petrologic and geochemical signatures, deformational style and orogenic evolution need to be clarified. Few papers focusing on the provenance and evolution of the Cordillera Frontal metamorphic rocks were published (Gregori et al., 1997, Basei et al., 1998, López et al., 1999, Vujovich and Gregori, 2001 and literature cited therein). Detailed studies about the petrology and geochemistry of the protoliths, and analysis of their deformational style would give clues about the Chilenia terrane. The aim of this paper is to characterize the stratigraphical configuration, geochemical signature and provenance of the Guarguaráz Complex rocks, which is supposed to be part of the Chilenia terrane.

Geological Setting

The Cordillera Frontal basement conforms a north-northeast belt, developed from Río Tunuyán to Río Mendoza. The study area extends from 33°18' to 33°21'S and from 69°25' to 69°30'W (Fig. 2). These rocks were

mapped by Stappenbeck (1917) and Polanski (1958, 1972) and assigned to the Neoproterozoic and Lower Paleozoic. In the Río de las Tunas area, the metasedimentary rocks include quartz-micaceous and biotite-garnetiferous schists, marbles and metapelites. They belong to marine environments of carbonatic and siliciclastic platforms, and slope facies (Gregori et al., 1997). Mafic and ultramafic bodies are emplaced through northeast trending faults, whereas metabasaltic dykes cut the metasedimentary sequences. Sedimentary and volcanic rocks were metamorphosed under greenschist, amphibolite and granulite facies (Ruviños et al., 1997). Deformation produced schistosity, crenulation, mineral lineations, dynamic recrystallization and porphyroblast rotations. López et al. (2001) assigned this assemblage to the Guarguaráz Complex. Preliminary K/Ar and Rb/Sr dating of the Guarguaráz Complex (Dessanti and Caminos, 1967, Caminos et al., 1979, and Basei et al., 1998), can be grouped in two periods: the older one with ages from Proterozoic to Lower Paleozoic (780 to 463 Ma) and a younger one with Middle Paleozoic ages (445 to 317 Ma). Ramos and Basei (1997) obtained U/Pb ages of 1069±36 and 1081±45 Ma in gneisses from Cordón del Portillo, which point towards Grenvillian ages. Sm/Nd model ages of 1427 to 1734 Ma in gneisses and schists, and 577 to 330 Ma in amphibolites, allowed Basei et al. (1998) to propose a Laurentian source for the protoliths of the Cordillera Frontal basement.

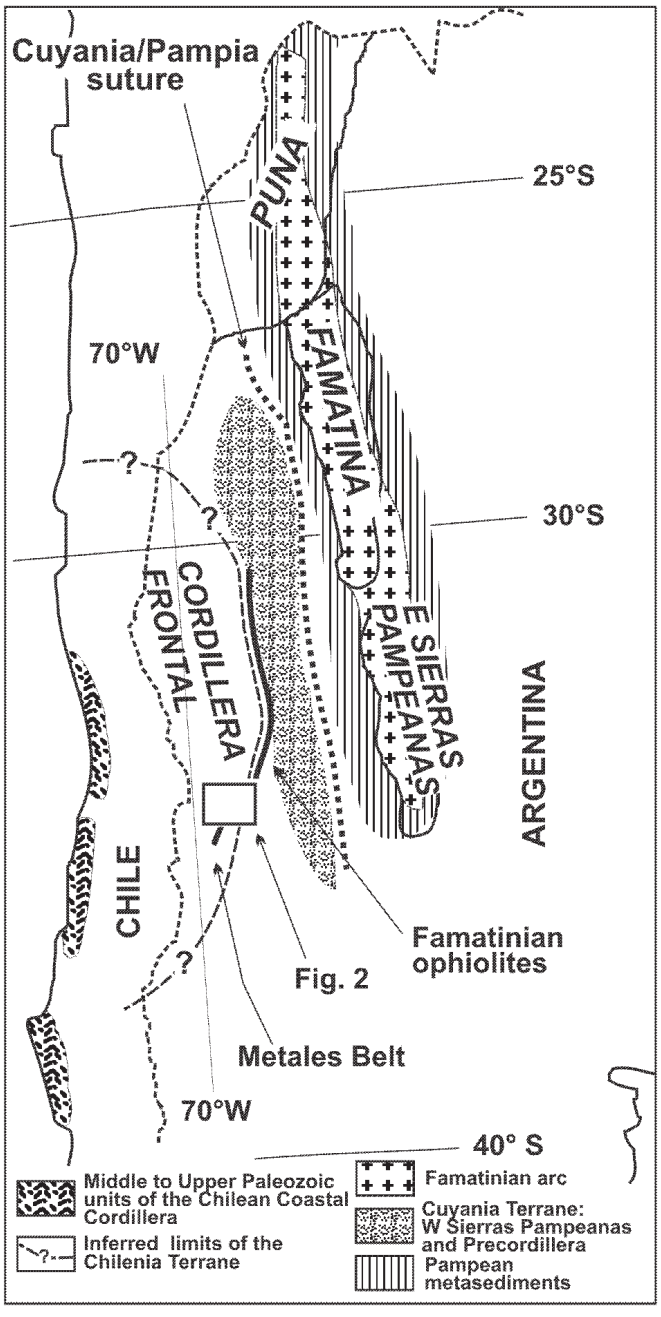

Fig. 1. Geological configuration of western Argentina and Chile, displaying distribution of Paleozoic units, terranes and sutures.

Carboniferous marine sediments are thrusted on or lay uncomfortably over the metamorphic rocks. Felsic sub-volcanic bodies and dikes intruded during Permo-Triassic times.

Petrology and Geochemistry of the Guarguaráz Complex

Geological arrangements recognized in the Río de las Tunas area, permit to divide the Guarguaráz Complex into three lithological assemblages: (1) Metasedimentary assemblage (MA), (2) Sub-volcanic and volcanic assemblage (SV-VA), and (3) Ultramafic bodies (UM).

Metasedimentary assemblage (MA)

Sequences derived from sedimentary rocks conform almost all the mapped area, from Loma del Medio to Los Tábanos Stock (Fig. 2). The MA is constituted by metaclastic and metacarbonatic associations, which include four different facies with transitional contacts: (a) Micaceous and quartzitic schists, (b) Metapelites, (c) Marbles, crystalline limestones and calcareous metasiltstones, and (d) Metacherts.

Micaceous and quartzitic schists: Micaceous schists are the dominant facies, whereas the quartzitic schists conform parts of the Cuchilla de Guarguaráz and Cuchilla de las Leñas. Transition from quartzitic to micaceous schists was recognized northwest of Refugio El Cóndor, whereas in Quebrada Confusión contact is by fault. In the eastern side of the Cuchilla de Guarguaráz, micaceous schists pass transitionally to calcareous schists and siltstones and finally to crystalline limestones. Between Arroyo Ordenes and Arroyo Gateado Overo small banks of crystalline limestones, amphibolites and metapelites are interbeded. The quartzitic schists display rhythmically alternating

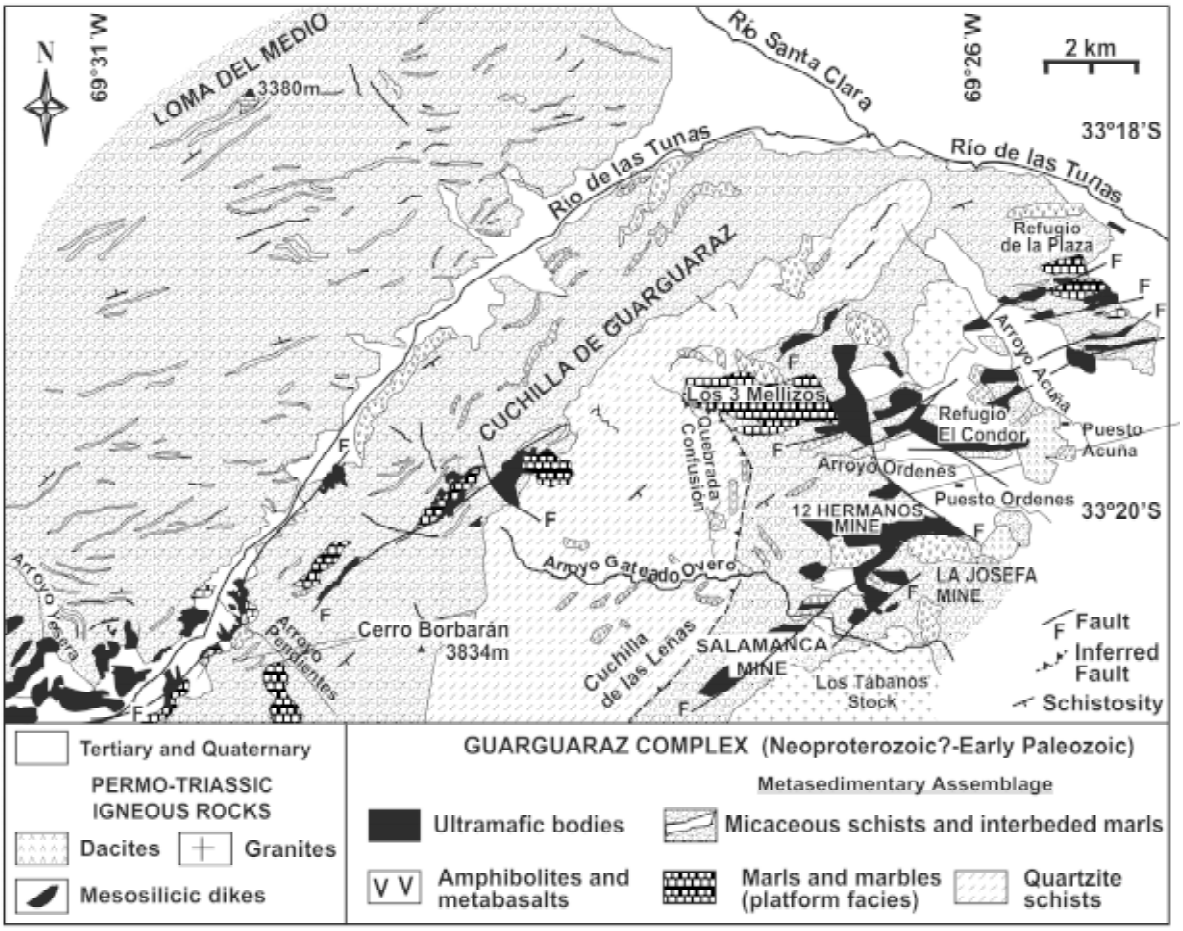

Fig. 2. Geological map of the Cuchilla de Guarguaráz.

banks of quartz-rich and metapelitic layers, conforming a more than 500 m-thick sequence. Lamination, cross stratification and festoons indicate paleoflow from northeast.

Quartz, muscovite, biotite, alkaline feldspar, plagioclase, amphibole, opaque minerals, garnet and chlorite compose the schists. Accessory minerals are zircon, calcite, hematite, epidote and apatite. Organic matter is present as inclusions or thin microfolded laminas. These rocks were metamorphosed under the quartz-albite-epidote-almandine subfacies of the greenschist grade (Turner and Verhoogen, 1975).

All rocks display a conspicuous northeast trending millimeter foliation (S1) sub-parallel to bedding (S0), related to the main phase of deformation (Fig. 2).

Two generations of biotite can be recognized: a chloritized biotite oriented in S1 foliation and a strong pleochroic biotite accompanied by muscovite oriented with S2 foliation. Rounded garnet and alkaline feldspar porphyroblasts display helicitic syn-kinematic textures. Post-kinematic garnet and neoformed dark biotite are related to the Triassic intrusions.

Metapelites: Metapelites are restricted to the Cuchilla de Guarguaráz summit and the Arroyo Pendientes. They show a laminated and microfolded texture, composed by organic matter, brown-reddish biotite, quartz, calcite and epidote.

Marbles, crystalline limestones and calcareous metasiltstones: Marbles and crystalline limestones cropping out in Los 3 Mellizos conform a 350 m-thick sequence dipping to the southeast. They pass transitionally to calcareous schists and mica-schists. Cross-stratification and festoons indicate paleoflow from east and southeast. Millimeter to 10 cm-thick laminated mudstones passing upwards to 2 m-thick calcareous banks, represent bars. In the granoblastic layers, the rock is composed by calcite, dolomite, opaque minerals and quartz, while crenulated biotite, tremolite and organic matter conform lepidoblastic and nematoblastic layers.

Metacherts: Metacherts appear in the Arroyo Gateado Overo, interbeded in the micaceous schists and metapelites. Dark layers 1.5 m thick constitute them, displaying a banded texture with mosaic quartz, hornblende, magnetite and minor biotite, muscovite and epidote.

Geochemistry and provenance

Twenty-three samples of the MA were analyzed for major and trace elements, using XRF, at the University of Barcelona and ACTLABS, whereas 7 samples were analyzed by REE, using INAA. Selected results are listed in table 1.

The MA is chemically classified as greywackes, subgreywackes, lutites-pelites and limestones-dolostones in the $Al_2O_3+Fe_2O_3$–SiO_2–MgO+CaO diagram of Pettijohn et al. (1987). The micaceous and quartzitic schists plot in the greywacke, lithic arenite and arkose fields of the log SiO_2/Al_2O_3 –log Na_2O/K_2O diagram of Pettijohn et al. (1987). The Zr–15*Al_2O_3–300*TiO_2 diagram of Garcia et al. (1994) indicates that greywackes, subgreywackes and lutites conform a continuous trend extending from Al-rich shales towards mature sandstones (Fig. 3a). Abundance of Al_2O_3, CaO, Na_2O and K_2O, represented in the Nesbitt and Young (1996) diagram, is consistent with weathering of plagioclase-alkaline feldspars to form illite-sericite. Low MgO, Fe_2O_3 and TiO_2 contents suggest no contribution from mafic source. The concentration of K and Rb are similar to the upper crustal rocks (Taylor and McLennan, 1985). On a Th/Sc vs. Cr/Th diagram (Totten et al., 2000), the MA rocks plot near the average of upper continental crust, discarding a two-component mixing model between felsic and mafic end members.

Tectonic setting

Major elements analyses: The diagram of Bathia (1983) indicates a passive margin origin. According to Roser and Korsch (1986) classification, which uses SiO_2/Al_2O_3 vs. K_2O/Na_2O, samples of the MA are PM (passive margin) or ACM (active continental margin) derived (Fig. 3b). Using the discriminant functions of Roser and Korsch (1988), designed to discriminate between four sedimentary provenance types, the majority of the MA rocks plot within the fields P4 (granitic-gneissic or sedimentary source, similar to PM-derived) and P2 (mature island arc, similar to ARC-derived), supporting the interpretation that they derived from a craton interior or a recycled orogenic terrane.

Normalized multi-element plots: Upper continental crust-normalized plots (Floyd et al., 1991) were used to discriminate the tectonic setting of the MA. The following source-distinguishing anomalies were recognized: (1) Nb/Nb*: 0.34–0.77, typical of PM or CAAM settings, (2) V, Cr, Ni, Ti and Sc anomalies <1, characteristic for PM environments, and (3) Sr and P anomalies <1, typical of PM (Fig. 3c)

Rare earth elements analyses: In a chondrite-normalized diagram (Fig. 3d), the MA rocks show similar REE patterns to PAAS (Post-Archean average Australian sedimentary rocks). Subgreywackes and siltstones are LREE enriched relative to HREE, displaying flat or nearly flat HREE patterns, with small negative Eu anomalies. This suggests that sediments derived from old upper continental crust and/or differentiated arc material compose the MA. According to McLennan et al. (1990) these provenance components are found in several basin types, but rarely in fore-arc settings. Based on other geochemical and petrographical data discussed herein, we considered that the MA is derived from old mature upper continental crust.

Sub-volcanic and volcanic assemblage (SV-VA)

Foliated and folded basic rocks, emplaced as dikes, domes, lava flows and sills constitute the SV-VA. Basic dikes are preferentially emplaced in the micaceous schists (Fig. 2). Between Salamanca and 12 Hermanos Mines, crops out a 200 m-long and 20 m-wide dykes, northeast oriented and foliated according to the MA. Westward of Salamanca Mine, basic dykes display radial arrangements from a major amphibolitic body. Several irregular ellipsoidal basic domes are associated to ultramafic bodies, being the best exposures located between Salamanca and 12 Hermanos Mines. They follow the regional foliation and are disposed in a sub-vertical position. Several small sills, 0.30–1 m thick, were recognized in Quebrada Confusión and Refugio de la Plaza areas, interbedded in the micaceous schists and folded according to the MA structure. Along the western flank of Cuchilla de Guarguaráz, 30 m thick sills are emplaced concordantly within the schistose sequence.

Petrography: SV-VA rocks are petrographically amphibolites. They display a banded texture (S1), formed by nematoblastic and granoblastic layers with ortho- and clino-amphiboles (anthophyllite, hornblende and tremolite), plagioclase (andesine), epidote, sphene, garnet, chlorite, quartz and opaque minerals. Two generations of tremolite were recognized: the older is coeval with hornblende and oriented with S1, while the younger cuts hornblende and foliation S1.

Geochemistry and tectonic setting

Major and trace elements, and REE were analyzed in 15 and 9 samples, respectively. Representative analyses are reported in table 1.

Major elements analyses: Metabasites from the SV-VA classify mainly as picrobasalts and basalts in the TAS diagram of LeBas et al. (1986). Rocks are subalkaline and display a tholeiitic trend in the Irvine and Baragar (1971) silica-alkali and AFM plots (Fig. 4a). They show strong negative correlation between TiO_2, Fe_2O_3, MnO, Na_2O and P_2O_5 against MgO on Harker-type diagrams. Positive

correlation can be observed between MgO and Cr, Ni and Co. These tendencies indicate that all samples belong to a unique magmatic cycle.

Normalized multi-element plots: Plotted in a transition metal diagram normalized to primitive mantle (Sun, 1982), SV-VA rocks display similar patterns to the NMORB (Fig. 4b). Metabasites plot mostly in the EMORB field (Fig. 4c–d) on a Th-La diagram (Gill, 1981) and in the Th-Hf/3-Ta ternary diagram of Wood (1980).

Rare Earth Elements analyses: The Guarguaráz Complex amphibolites show low concentration in REE (52–135 ppm). Chondrite-normalized REE patterns show 15 to 70 times LREE enrichment, with La_N/Yb_N: 0.7–3.3. Small positive Eu anomalies can be recognized in samples M30, N12, N24, N89 and N95, due to enrichment in plagioclase (Fig. 4e). The lowest La_N/Yb_N ratio belongs to sample GO17, which classify as N-MORB, whereas the other samples are similar to E-MORB.

Ultramafic bodies (UM)

Ultramafic bodies were fault-emplaced into the MA sequences following parallel belts along the Cuchilla de Guarguaráz, with ophicalcites, rodingites and mylonites associated in the borders.

The UM can be divided in three segments: (1) eastern segment, located between Arroyo Ordenes and Refugio de la Plaza; (2) central segment, comprising the Salamanca and 12 Hermanos Mines area, and (3) western segment, along Río de las Tunas (Fig. 2). There are not original magmatic textures in these bodies; they only show 'mesh' and interpenetrative textures conformed by serpentine and scarce relictic olivine and diopside. Diopside cores are surrounded by serpentine, talc and calcite. Tremolite, chlorite and opaque minerals constitute minor phases.

Geochemistry

Twelve samples were analyzed by major and trace

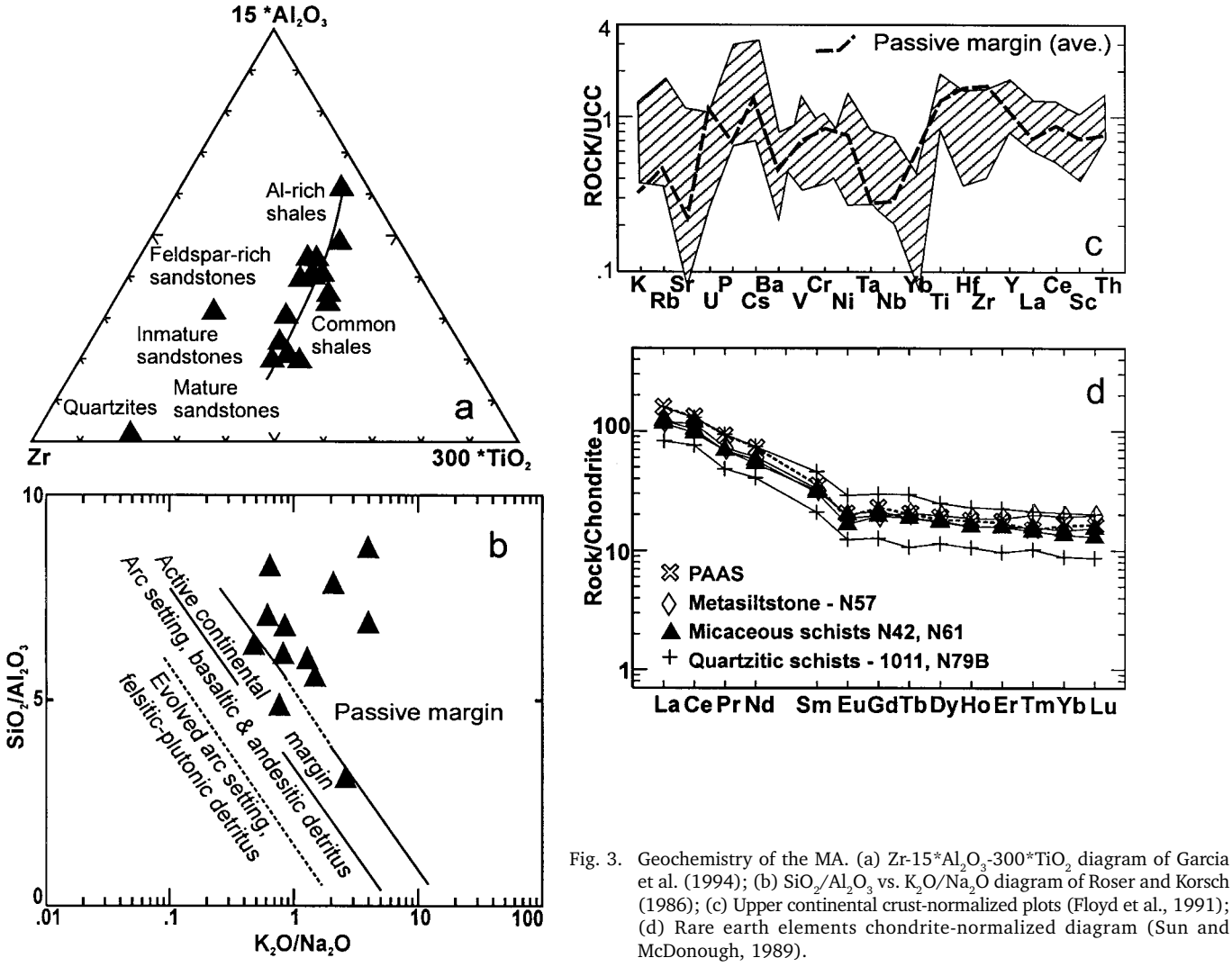

Fig. 3. Geochemistry of the MA. (a) Zr-15*Al_2O_3-300*TiO_2 diagram of Garcia et al. (1994); (b) SiO_2/Al_2O_3 vs. K_2O/Na_2O diagram of Roser and Korsch (1986); (c) Upper continental crust-normalized plots (Floyd et al., 1991); (d) Rare earth elements chondrite-normalized diagram (Sun and McDonough, 1989).

Table 1. Representative chemical analyses of the metasedimentary assemblage, the sub-volcanic and volcanic assemblage and the ultramafic bodies.

	Marbles and calcareous schists			Micaceous schists				Quartzitic schists		Amphibolites					Ultramafic bodies				
Sample	GO-9	B04160292	A12B	N42	N78	N57	N61	1011297	N79B	A15	N24	GO-17	N89	N95	35260289	2120293	9120293	9260294	19010389
Analyst	Actlabs	Actlabs	Un Barcelona	Actlabs	Actlabs	Actlabs	Actlabs	Actlabs	Actlabs	Actlabs	Actlabs	Actlabs	Actlabs	Actlabs	Actlabs	Actlabs	Actlabs	Actlabs	Actlabs
SiO[2]	0.45	28.46	7.12	71.92	74.79	58.18	74.10	72.36	76.98	48.57	45.48	43.60	48.63	49.12	43.16	26.17	25.86	39.60	46.12
TiO[2]		0.23	0.01	0.68	0.43	0.89	0.42	0.99	0.35	1.49	1.88	1.47	1.60	1.59	0.20	1.78	1.30	0.01	0.06
Al[2]O[3]	0.09	6.96	0.75	11.46	9.61	18.83	10.87	10.62	8.86	14.44	16.20	14.60	15.33	14.39	2.13	19.72	4.75	0.90	1.18
Fe[2]O[3]	1.79	4.32	4.26	4.83	5.49	9.51	6.65	5.67	5.94	11.37	12.92	12.50	11.85	11.82	10.19	20.19	15.72	7.28	9.44
MnO	0.19	0.19	0.43	0.10	1.08	0.16	0.22	0.10	0.09	0.17	0.20	0.22	0.16	0.21	0.02	0.19	0.16	0.08	0.06
MgO	19.85	6.80	2.13	1.59	3.06	2.67	2.20	1.79	1.91	7.99	6.77	9.05	6.91	7.34	41.03	21.23	24.62	36.76	42.87
CaO	32.61	24.72	50.14	1.70	0.31	0.23	0.16	0.89	0.09	8.84	12.32	14.4	11.89	11.79	3.06	0.19	8.29	2.44	0.52
Na[2]O	0.50	2.02	0.20	3.07	0.83	1.81	0.65	2.11	0.51	3.31	2.19	0.82	2.51	2.17	0.03	0.01	0.02	0.02	0.05
K[2]O	0.15	3.64	0.06	1.47	1.73	4.54	2.58	1.77	1.98	0.82	0.15	0.43	0.21	0.13	0.03	0.05	0.01	0.01	0.05
P[2]O[5]	0.10	0.25	0.06	0.15	0.13	0.12	0.11	0.19	0.08	0.16	0.17	0.11	0.15	0.30	0.07	0.13	0.49	0.01	0.01
LOI	43.97	21.98	37.89	1.94	1.98	3.18	2.27	1.67	2.45	3.21	2.26	2.89	1.18	1.72	1.15	10.35	17.56	12.88	0.61
TOTAL	99.70	99.57	103.05	98.91	99.44	100.12	100.23	98.16	99.24	100.37	100.54	100.09	100.42	100.58	101.07	100.01	98.78	99.99	100.97
Cr		73	506	44	45	84	45	63	33	380	74	310	192	359	1484	332	78	331	2510
Ni			583	25	29	42	23	26	24	121	89	138	104	145	1283	185	645	545	2157
Co		33.22	80.10	13.21	20.11	23.52	20.05	15.23	17.58	51.32	49.42	51.21	48.05	51.87	89.10	71.60	56.90	74.24	105.85
Sc				12	8	21	12	12	11	41	42	45	39	42	1	50	21	7	1
V		58.45	18.02	81.32	58.36	153.35	80.45	85.21	65.02	295.37	360.68	354.75	311.62	309.19	46.08	204.11	61.25	18.33	21.21
Cu			1.82	26.45	369.87	15.23	23.11	34.87	22.83	84.48	166.54	8.01	96.55	123.81	13.25	13.98		18.01	190.28
Pb		14	8	9	8	29		10	7	9	5	7	7	5	9			3	8
Zn		25.04	30.91	55.02	54.45	119.05		60.47	41.45	77.05	95.21	94.31	77.47	81.92	62.63	133.25	6.12	4.85	51.46
Sn			3.91	2.32	2.58	4.89	2.17	2.24	2.36	1.17	1.31	1.73	2.49	1.14		3.33		1.35	
Rb		70.98		64.23	65.56	202.47	124.59	70.78	77.21	34.73	4.18	8.15	2.64	3.53		56.60	15.50	21.12	
Cs				3.9	2.7	11.8	5.9	2.3	1.6	3.6		0.9	1.1	1.2				0.9	
Ba		270.69	111.91	306.08	381.26	544.78	355.58	227.41	350.78	254.03	4.53	43.74	24.27	71.88		83.46	9.85		
Sr		345.25	622.61	116.24	29.56	79.78	44.79	79.16	17.54	251.04	265.64	412.75	233.07	256.96		11.80	1.50		
Ga		8.85	3.53	14.14	16.52	28.75	15.45	15.86	13.78	19.99	23.04	23.91	21.21	20.84		2.20	0.40	5.04	
Ta		1.26		0.91	0.73	1.42	0.61	1.24	0.65	0.48	0.48	0.31	0.47	0.63	1.20	0.10			0.30
Nb		11.43	5.21	7.14	4.36	13.89	5.24	11.80	4.21	3.28	3.68	1.94	3.33	3.89		0.80	1.01		
Hf				5.4	2.3	4.2	2.1	9.2	1.9	2.6	3.0	2.6	2.5	2.6	35.1	22.4	2.4	8.2	2.6
Zr		80.46	23.21	189.45	80.56	142.12	79.34	321.12	65.23	96.04	100.95	85.09	85.00	93.14	98.22	7.50	115.90	16.04	5.01
Y		9.22	8.91	25.33	19.55	30.41	27.47	36.32	16.47	24.14	28.62	33.90	24.21	26.24	15.11	10.21	5.14	5.10	15.08
Th		3.19		8.21	7.92	14.63	8.24	9.40	6.48	0.61	0.62	0.36	0.59	0.58		0.53	1.27	1.01	
U				2.1	1.1	2.5	1.5	2.2	0.8	0.2	0.1	0.1	0.2	0.1	9.3	8.7	30.7	4.5	10.1
La				27.62	18.94	29.90	29.11	37.31	19.62	6.65	7.19	3.84	6.43	6.38	0.50	2.20	17.30	11.01	0.48
Ce				59.21	34.12	72.33	63.34	79.78	46.60	17.41	19.03	11.21	16.97	17.03	37.04	82.14	886.20	6.02	5.20
Pr				6.55	4.01	7.14	6.55	8.91	4.57	2.42	2.68	1.74	2.34	2.42					
Nd				25.11	16.72	29.41	26.82	34.81	19.21	13.19	14.43	10.32	12.71	12.97	9.40	12.01	107.84	4.52	5.50
Sm				4.90	2.91	5.22	4.71	7.01	3.21	3.38	3.81	3.34	3.30	3.38	0.30	0.21	3.04	2.56	0.91
Eu				1.16	0.69	1.14	0.96	1.68	0.72	1.31	1.46	1.24	1.31	1.36	0.40	0.24	4.22	3.21	0.32
Gd				4.41	2.84	4.22	4.32	6.11	2.60	3.52	4.19	4.02	3.45	3.61	3.45	23.24	9.80	7.45	0.55
Tb				0.72	0.52	0.82	0.74	1.12	0.45	0.72	0.83	0.89	0.71	0.72	4.60	47.50	41.90	20.48	2.13
Dy				4.50	3.21	5.23	4.42	6.30	2.91	4.45	5.29	6.11	4.48	4.49		4.33	6.15	5.14	
Ho				0.91	0.72	1.10	0.94	1.31	0.64	0.88	1.07	1.31	0.92	0.93	4.80	20.70	41.10	32.33	6.11
Er				2.62	1.84	3.21	2.63	3.72	1.62	2.47	2.96	3.68	2.47	2.59	1.50	5.10	16.23	8.21	0.12
Tm				0.45	0.29	0.53	0.37	0.54	0.26	0.36	0.44	0.57	0.37	0.38	0.20	0.63	1.78	1.21	0.15
Yb				2.50	1.72	3.41	2.31	3.50	1.50	2.18	2.75	3.72	2.22	2.42		4.30	17.80	8.01	
Lu				0.39	0.26	0.52	0.33	0.51	0.22	0.31	0.40	0.55	0.33	0.36	0.30	0.60	3.90	1.21	0.30

Major elements in wt. percent, trace and REE in ppm.

elements, whereas 7 by REE. Representative analyses are reported in table 1.

Major elements analyses: Ultramafic rocks have SiO_2: 36.8–47.3 wt.%, Al_2O_3: 0.84–5.39 wt.% and MgO: 26.70–38.21 wt.%. Samples 2120293 and 9120293 have anomalous concentrations of SiO_2, Al_2O_3 and Fe_2O_3 due to alteration, while TiO_2 is exceptionally enriched (1.78 and 1.3 wt.%, respectively) possibly due to abundance of illmenite. All samples are plagioclase, pyroxene and olivine-normative, with Mg#: 65–96 (calculated as Mg# = 100*Mg/(Fe+Mg) following Middlemost, (1989)). According with the CIPW calculation samples of the eastern and central segments have 3.77 to 17.77 wt.% of plagioclase, plotting in the melagabbroids field on a Px-Pl-Ol diagram. Samples from the Río de las Tunas segment have 0.18–2.9 wt.% of plagioclase, plotting in the plagioclase-bearing ultramafic rocks field. UM classify mainly as lherzolites in the Opx-Cpx-Ol diagram for ultramafic rocks (Fig. 5a). Most samples plot in the picrite basalt field in alkalies-silica diagram of Cox et al. (1979), whereas in the AFM diagram of Irvine and Baragar (1971) they follow a tholeiitic trend. The Al_2O_3–Mg# diagram indicate that UM rocks are comparable with those from the Hess Deep abyssal peridotites (Gillis et al., 1993).

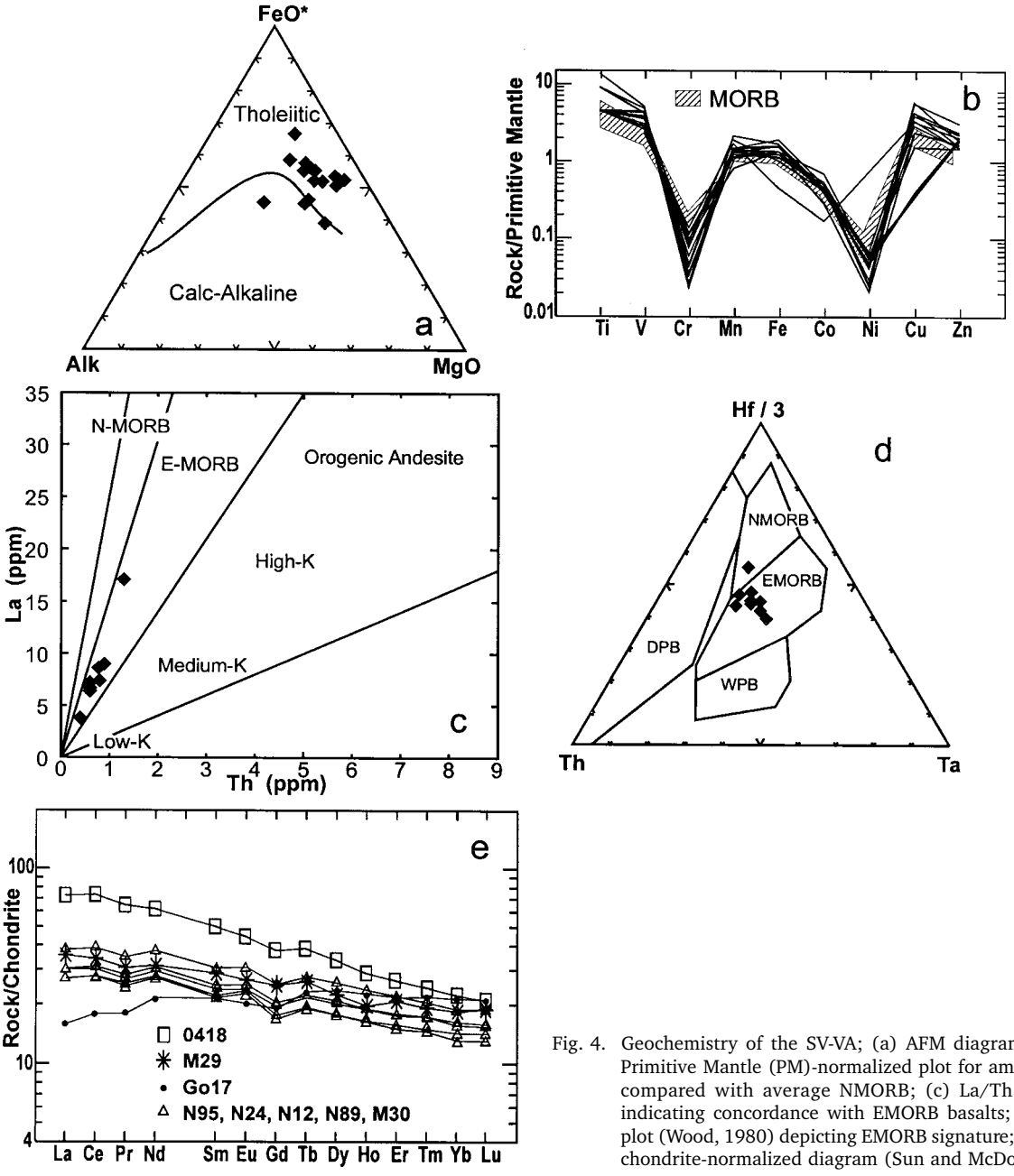

Fig. 4. Geochemistry of the SV-VA; (a) AFM diagram; (b) Transition metal Primitive Mantle (PM)-normalized plot for amphibolites of the SV-VA, compared with average NMORB; (c) La/Th diagram (Gill, 1981), indicating concordance with EMORB basalts; (d) Hf/3-Ta-Th ternary plot (Wood, 1980) depicting EMORB signature; (e) Rare earth elements chondrite-normalized diagram (Sun and McDonough, 1989).

Rare Earth Elements analyses: In a chondrite-normalized REE spidergram (Fig. 5b), four groups can be recognized according their REE enrichment. Samples 35260289 and 7130293 (Arroyo Yesera) display nearly flat patterns 5 to 10 times enriched, similar to samples of the Ussuit Komatiite (Kalsbeek and Manatschal, 1999). Samples 9120293, 9260294 and N84F (Río de las Tunas) are 30 to 100 times enriched, and slightly LREE depleted. Eu negative anomalies (Eu/Eu*) vary between 0.32 and 0.64 reflecting some plagioclase fractionation. Samples 15010389 and 2120293 (Arroyo Yesera) have La_N/Lu_N between 3 and 10. The first one is 200 times enriched, displaying a positive Eu anomaly, typical of plagioclase-rich gabbro. Sample 2120293 has La_N/Lu_N of 10, possible due to retention of garnet in the source; and pronounced Eu/Eu* (0.42), indicative of an important plagioclase fractionation.

Structure and Deformation of the Guarguaráz Complex

The Guarguaráz Complex conforms a decakilometer-scale anticline to regional axis 3º/N47º. In the eastern flank of this structure, schistosity S1 dips to the southeast, whereas the northwestern side dips to the north or northwest (Fig. 2). The Guarguaráz Complex overthrusts tertiary sediments to the east in a structure known as Espolón de la Carrera (Polanski, 1958), and is overthrusted by folded Carboniferous rocks to the west.

Several SE vergent slices of ten- to thousand-meters thick, including folded metasedimentary and metavolcanic sequences are tectonically imbricated. Thrust sheets transporting mafic sills and domes and ultramafic bodies are exposed predominantly in the eastern flank of Cuchilla de Guarguaráz and along Río de las Tunas (Fig. 2).

The MA rocks, deposited in passive margin environments, were progressively deformed and metamorphosed in an accretionary prism at an active margin. During this process, S1 foliation and decameter to hundred-meters folding were developed, while crenulation and S2 foliation were developed later. Radiometric dating using Rb/Sr and K/Ar isotopes by Dessanti and Caminos (1967), Caminos et al. (1979) and Basei et al. (1998) on biotite and amphibole indicate ages from 425 to 355 Ma for this deformation. Coevally, slices of ultramafic and mafic rocks were tectonically emplaced into the metasedimentary sequences.

After Devonian, extensional faulting and subsidence of the western margin of Gondwana conditioned the deposition of Carboniferous marine sediments over the Guarguaráz Complex. Deformation during Permian generated folding of the Carboniferous sediments, and northeast and northwest faulting in the Guarguaráz Complex, were felsic dykes were emplaced. Andean

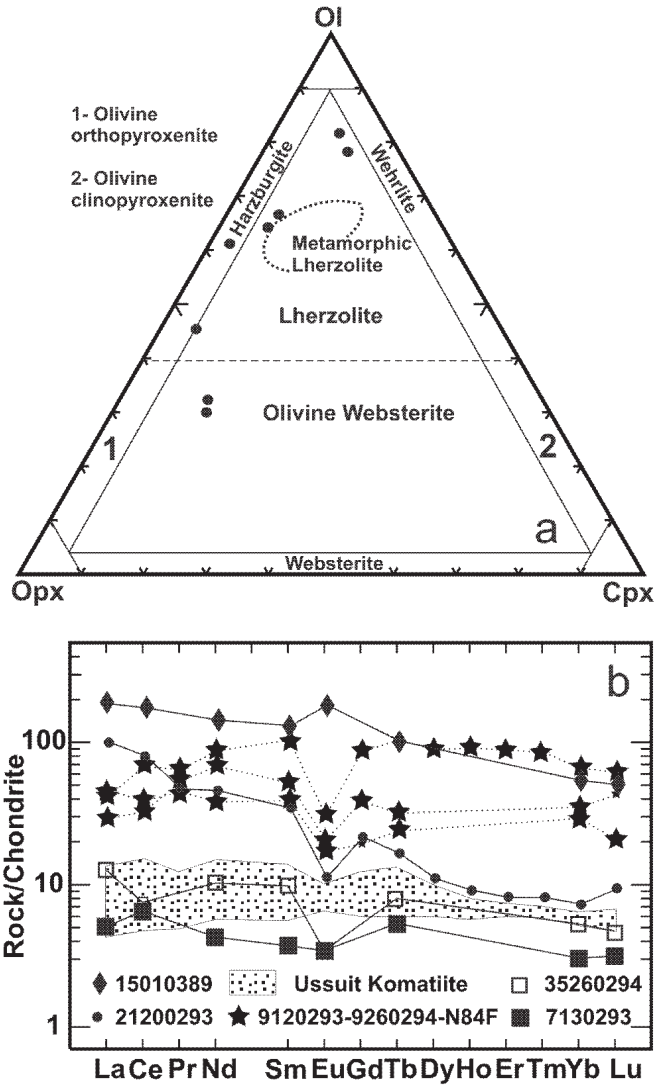

Fig. 5. Geochemistry of the UM. (a) Opx-Cpx-Ol diagram; (b) Rare earth elements chondrite-normalized diagram (Sun and McDonough, 1989).

deformation is characterized by reactivation of northeast structures with strike-slip and thrust components.

Correlations

The structural style of the Guarguaráz Complex resemble to the Lower Paleozoic sequences of western Precordillera, with E-vergent thrusts and W-vergent back thrusts. The continuity of the Cordillera Frontal mafic and ultramafic belt along the western Precordillera was analyzed and confirmed by several authors (Zardini, 1962; Caminos, 1993; Haller and Ramos, 1984, among others). In addition to the ultramafic belt continuity, their host units in western Precordillera (Bonilla, Cortaderas and Alcaparrosa Formations; Cucchi, 1972; Caminos, 1993; Davis et al., 1999) display similar characteristics to the

Guarguaráz Complex. Furthermore, the Bonilla Formation holds physical continuity with the Guarguaráz Complex.

Davis et al. (1999) interpreted the Lower Paleozoic geological history of the Cortaderas Formation as developed in four successive stages from Lower Cambrian to Middle Devonian. They interpreted an initial extensional setting (576±17 Ma) in a passive margin as related to the opening of a narrow ocean between the Precordillera and Chilenia Terranes. During Late Ordovician times (450±20 Ma) a westward-directed subduction in the Chilenia eastern margin was also active, although no evidence of arc was recognized (Davis et al., 1999). Closure of this narrow basin continues during Silurian and Early Devonian (418±10 Ma), ending with deformation and metamorphism at Middle Devonian times (384.5±0.5 Ma, Davis et al., 1999, 2000).

Middle Silurian to Devonian K/Ar and Ar/Ar ages (437.4–353.1 Ma) for the deformation and metamorphism of the Bonilla Formation were obtained by Cucchi (1971), Buggisch et al. (1994) and Davis et al. (1999). These ages are coincident with those of the Cortaderas Formation and the Guarguaráz Complex. Similar ages (377±0.5 Ma) of deformation were also obtained by Davis et al. (1999) in the Guarguaráz Complex rocks cropping out in Cordón de Portillo (Cordillera Frontal).

Cambro-Ordovician sequences, deposited as platforms and turbiditic facies in extensional settings are represented by the Yerba Loca, La Invernada and Don Polo Formations in central and western Precordillera. They include ultramafic bodies and interbedded pillow lavas related to oceanic crust development. These units display a low-grade metamorphism and were deformed during Late Ordovician to Silurian times (Rubinstein et al., 1998). Based on previous radiometric dating and structural considerations, Gosen (1997) considers the low-grade metamorphic overprint and deformation of these units as developed between Late Silurian and post-Early Devonian times.

Eastwards of Precordillera, in the Puna, Famatina System, western Sierras Pampeanas and Sierras de San Luis, the Ordovician to Devonian times are represented by the Famatinian arc (Figs. 1 and 6). It is constituted by calc-alkaline volcanic rocks interlayered within marine

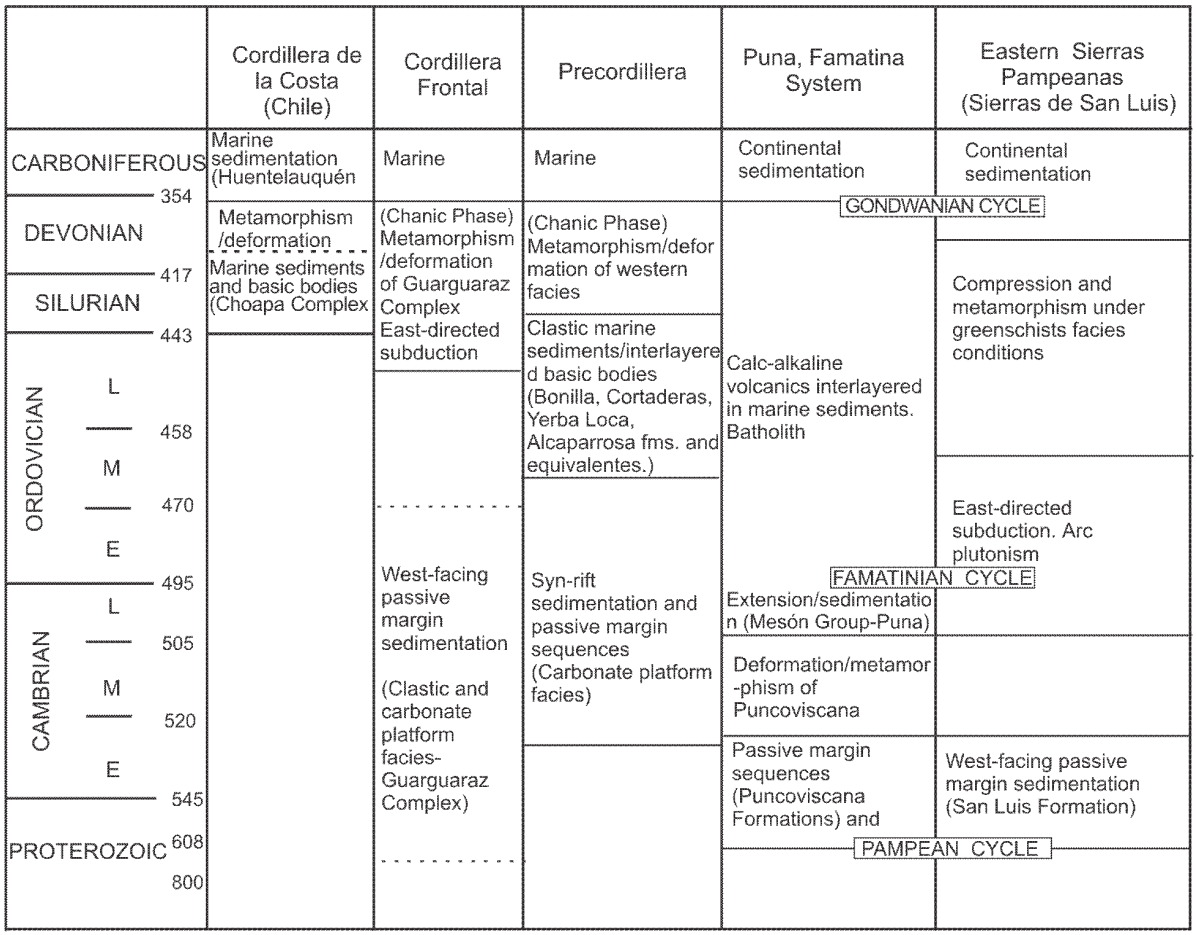

Fig. 6. Stratigraphical correlation chart of Neoproterozoic to Late Paleozoic units and deformation/metamorphic events for western Argentina regions and Central Chile.

sediments, emplacement of plutonic rocks and low- to high-grade metamorphism of Cambro-Ordovician successions (Pankhurst and Rapela, 1998).

In Sierras de San Luis, González et al. (2002) recognized a Pampean (530–483 Ma) metamorphism-deformation episode superimposed by a Famatinian metamorphism (475–458 Ma). Gosen et al. (2002) described the Sierras de San Luis evolution as conformed by several steps, initiating as a west-facing passive margin started at ~608 Ma. Sedimentation was continuous up to Early Cambrian without evidence of Pampean compression. Famatinian arc plutonism, related to east-directed subduction, started ~500 Ma and continued to ~460 Ma. Arc plutonism was followed by compression and metamorphism under greenschists facies conditions during Late Ordovician–Early Devonian.

Within the Chilean Coastal Cordillera, north of 34°S, crop out Silurian and Early Devonian fossiliferous rocks associated with oceanic mafic and ultramafic rocks, metamorphosed during the Devonian-Carboniferous transition (380 to 311 Ma, Hervé et al., 1984). Between 31° and 32°S, in the Chilean Coastal Cordillera crop out phyllites, amphibolites, quartz-micaceous schists and rarely marbles, assigned to the Choapa Formation. The metamorphic episode was dated 359±36 Ma (Rivano and Sepúlveda, 1991), equivalent to deformation metamorphism ages of the Guarguaráz Complex. This unit shows a gradual structural transition with the Arrayanes Formation, composed by turbiditic metagreywackes and metapelites affected by low-grade metamorphism. Rivano and Sepúlveda (1991) interpreted both units as an accretionary prism. The unmetamorphosed marine Huentelauquén Formation (Carboniferous) covers unconformably the metamorphosed rocks. A similar relationship was also recognized between the Guarguaráz Complex and Fm Alto Tupungato in the Guarguaráz area (Fig. 6).

Conclusions

The protoliths and the structural arrangement of the Guarguaráz Complex indicate two different stages in its evolution: the first one is characterized by extensional conditions in a marine passive margin open to the west. According to geochemical data, these sediments were derived through erosion of granites or felsic gneisses of a mature cratonic continental basement. During deposition, N and E-MOR basalts were interbeded in the sequences due to generation of oceanic crust during basin development. Extensional conditions are similar to those of the Cortaderas and Bonilla areas. Rb/Sr and K/Ar ages ranging from 780 to 463 Ma obtained by Caminos et al. (1979) and Davis et al. (1999) are indicative of this stage.

The second stage represents compressional conditions, which are related to progressive deformation and metamorphism of the sedimentary rocks, together with the emplacement of slices of oceanic crust, conforming an accretionary prism. This stage represents switching from extensional to compressional conditions, during Late Devonian. The compressional episode was also recognized in the western Precordillera and is associated with juvenile eastward-directed subduction. Deformation and metamorphism is related to the Chanic deformational phase of the Famatinian Orogeny (Fig. 6).

The Guarguaráz Complex and equivalent units in western Precordillera and also in the Chilean Coastal Cordillera share common evolutional stages, widely represented along the western Gondwana margin. These evidences imply that Chilenia is not an allochthonous terrane to Gondwana, but a portion of its Early Paleozoic margin. Regional configuration indicates that the Guarguaráz Complex and equivalent units represent the accretionary prism of the Famatinian arc.

Acknowledgments

G. Vujovich and L.A.D. Fernandes are gratefully acknowledged for the kind invitation to the international symposiun on the Acrescao do Microcontinente Cuyania a Proto-Margem do Gondwana held in Porto Alegre, Brazil.. Helpful comments by V. Ramos and R. Varela during the symposium are acknowledged. We thank M. L. de Luchi, G. Vujovich and H. Bahlburg for the observations, comments and suggestions, which contributed greatly to improving the interpretations. Fieldwork was partially financed by CONICET.

References

Astini, R., Benedetto, J. and Vaccari, N. (1995) The early Paleozoic evolution of the Argentine Precordillera as a Laurentian rifted, drifted and collided terrane: a geodynamic model. Geol. Soc. Amer., Bull., v. 107, pp. 253-273.

Basei, M., Ramos, V., Vujovich, G. and Poma, S. (1998) El basamento de la Cordillera Frontal de Mendoza: nuevos datos geocronológicos e isotópicos. 10° Congr. Latinamer. Geol. and 6 Congr. Nac. Geol. Económica, Actas,2 , pp. 412-417.

Bathia, M. (1983) Plate tectonics and geochemical composition of sandstones. J. Geol., v. 9, pp. 611-627.

Buggisch, W., Gosen, W. von, Henjes-Kunst, F. and Krumm, S. (1994) The age of early Paleozoic deformation in metamorphism in the Argentine Precordillera-evidence of K-Ar data. Zentr. Geol. und Paläont., Teil 1: pp. 275-286

Caminos, R. (1993) El basamento metamórfico Proterozoico-Paleozoico inferior. In: Ramos, V. (Ed.), Geología y Recursos Naturales de Mendoza. 12° Congr. Geol. Argentino and 2° Congr. Explorac. Hidrocarburos., Relatorio, Cap. 1 (2), pp. 11-19.

Caminos, R., Cordani, U. and Linares, E. (1979) Geocronología y geología de las rocas metamórficas y eruptivas de la Precordillera y Cordillera Frontal de Mendoza. 2° Congr. Geol. Chileno, Actas, 1, pp. 43-61.

Cox, K., Bell, J. and Pankhrust, R. (1979) The interpretation of igneous rocks. George, Allen and Unwin, London, 450p.

Cucchi, R. J. (1971) Edades radimétricas y correlación de metamorfitas de la Precordillera, San Juan-Mendoza, República Argentina. Revista Asoc. Geol. Argentina, v. 26, pp. 503-515.

Cucchi, R. J. (1972) Geología y estructura de la Sierra de Cortaderas, San Juan-Mendoza, República Argentina. Revista Asoc. Geol. Argentina, v. 27, pp. 229-248.

Davis, J., Roeske, S., McClelland, W. and Snee, L. (1999) Closing the ocean between the Precordillera terrane and Chilenia: Early Devonian ophiolite emplacement and deformation in the southwest Precordillera. In: Ramos, V. and Keppie, J. (Eds.), Laurentia and Gondwana connections before Pangea. Geol. Soc. Amer., Spec. Paper, v. 336, pp. 115-138.

Davis, J., Roeske, S., McClelland, W. and Kay, S. (2000) Mafic and ultramafic crustal fragments of the southwestern Precordillera terrane and their bearing on tectonic models of the early Paleozoic in western Argentina. Geology, v. 28, pp 171-174.

Dessanti, R. and Caminos, R. (1967) Edades potasio-argón y posición estratigráfica de algunas rocas ígneas y metamórficas de la Precordillera, Cordillera Frontal y Sierras de San Rafael, provincia de Mendoza. Revista Asoc. Geol. Argentina, v. 22, pp. 135-162.

Floyd, P., Shail, R., Leveridge, B. and Franke, W. (1991) Geochemistry and provenance of Rhenohercynian synorogenic sandstones: implications for tectonic environment discrimination. In: Morton, A., Todd, S. and Haughton, P. (Eds.), Developments in Sedimentary Provenance. Geol. Soc. London, Spec. Pub., v. 57, pp. 173-188.

Garcia, D., Fonteilles, M. and Moutte, J. (1994) Sedimentary fractionations between Al, Ti and Zr and the genesis of strongly peraluminous granites. J. Geol., v. 102, pp. 411-422.

Gill, J. (1981) Orogenic andesites and plate tectonics. Springer, Berlin, 390p.

Gillis, K., Mevel, C., Allan, J., et al. (incl. Richter, C.) (1993) Proceedings of the Ocean Drilling Program, Initial Reports, Leg. 147: College Station, TX (Ocean Drilling Program), 366p.

González, P., Sato, A., Basei, M., Vlach, S. and Llambías, E. (2002) Structure, metamorphism and age of the Pampean-Famatinian Orogenies in the western Sierra de San Luis. 15° Congr. Geol. Argentino, Actas, 2, pp. 51-56.

Gosen, W. von (1997) Early Paleozoic and Andean structural evolution in the Río Jáchal section of the Argentine Precordillera. J. S. Amer. Earth Sci., v. 10, pp. 361-388.

Gosen, W. von, Loske, W. and Prozzi, C. (2002) New isotopic dating of intrusive rocks in the Sierra de San Luis (Argentina): implications for the geoynamic history of the Eastern Sierras Pampeanas. J. S. Amer. Earth Sci., v. 15, pp. 237-250.

Gregori, D., Ruviños, M. and Bjerg, E. (1997) Las metamorfitas del basamento de la Cordillera Frontal, entre el Río de las Tunas y el Ao. Barraquero, Provincia de Mendoza. 8° Congr. Geol. Chileno, Actas,2 , pp. 1295-1299.

Haller, M. and Ramos, V. (1984) Las ofiolitas famatinianas (Eopaleozoico) de las provincias de San Juan y Mendoza. 9° Congr. Geol. Argentino, Actas, 2, pp. 66-83.

Hervé, F., Kawashita, K., Munizaga, F. and Bassei, M. (1984) Rb-Sr isotopic ages from late Paleozoic metamorphic rocks of central Chile. J. Geol. Soc. London, v. 141, pp. 877-884.

Irvine, A. and Baragar, W. (1971) A guide to the chemical classification of the common volcanic rocks. Canadian J. Earth Sci., v. 8, pp. 523-548.

Kalsbeek, F. and Manatschal, G. (1999) Geochemistry and tectonic significance of peridotitic and metakomatiitic rocks from the Ussuit area, Nagssugtoqidian orogen, West Greenland. Precambrian Res., v. 94, pp. 101-120.

LeBas, M.J., LeMaitre, R.W., Streckeisen, A. and Zanettin, B. (1986) A chemical classification of volcanic rocks based on the total alkali silica diagram. J. Petrol., v. 27, pp. 745-750.

López, V., Gregori, D. and Migueles, N. (2001) Stratigraphy and structure of the Guarguaráz Complex, Frontal Cordillera, Argentina. Geol. Soc. Amer., Ann. Meeting, Boston. Abst. BTH 98, A-383.

López, V., Gregori, D., Migueles, N. and Dimartino, C. (1999) Nuevas facies en el basamento metamórfico de la Cordillera Frontal de Mendoza, Argentina. 14° Congr. Geol. Argentino, Actas, 1, pp. 141-144.

McLennan, S., Taylor, S., McCulloch, M. and Maynard, J. (1990) Geochemical and Nd-Sr isotopic composition of deep-sea turbidites: Crustal evolution and plate tectonic associations. Geochim. Cosmochim. Acta, v. 54, pp. 2015-2050.

Middlemost, E.A.K. (1989) Iron oxidation ratios, norms and the classification of volcanic rocks. Chem. Geol., v. 77, pp. 19-26.

Nesbitt, H.W. and Young, G.M. (1996) Petrogenesis of sediments in the absence of chemical weathering: effects of abrasion and sorting on bulk composition and mineralogy. Sedimentology, v. 43, pp. 341–358.

Pankhurst, R.J. and Rapela, C.W. (1998) The proto-Andean margin of Gondwana: an introduction. In: Pankhurst, R.J. and Rapela, C.W. (Eds.), The Proto-Andean margin of Gondwana. Geol. Soc., London Spec. Pub., v. 142, pp. 1-9.

Pettijohn, F., Potter, P. and Siever, R. (1987) Sand and Sandstones. Springer-Verlag, Berlin, 617p.

Polanski, J. (1958) El bloque Varíscico de la Cordillera Frontal. Revista Asoc. Geol. Argentina, v. 12, pp. 165-196.

Polanski, J. (1972) Descripción Geológica de la Hoja 24 a-b, Cerro Tupungato, (Provincia de Mendoza). Serv. Geol. Nac., Sec. de Estado de Minería, Buenos Aires. Boletín 165, 117p.

Ramos, V. and Basei, M. (1997) The basement of Chilenia: an exotic continental terrane to Gondwana during the early Paleozoic. In: Bradshaw, J. and Weaver, S. (Eds.), Intern. Conf. on Terrane Geology, Christchurch, Abst., pp. 140-143.

Ramos, V., Jordan, T., Allmendinger, R., Kay, S., Cortés, J. and Palma, M. (1984) Chilenia: un terreno alóctono en la evolución paleozoica de los Andes Centrales. 10° Congr. Geol. Argentino, Actas, 2, pp. 84-106.

Ramos, V., Jordan, T., Allmendinger, R., Mpodozis, C., Kay, S., Cortés, J. and Palma, M. (1986) Paleozoic terranes of the central Argentine-Chilean Andes. Tectonics, v. 5, pp. 855-888.

Ramos, V., Vujovich, G.I and Dallmeyer, R.D. (1996) Los klippes y ventanas tectónicas preándicas de la Sierra de Pie de Palo (San Juan): Edad e implicaciones tectónicas. 13° Congr. Geol.

Argentino and 3° Congr. Explorac. Hidrocarburos, Actas, 5, pp. 377-391.

Rivano, S. and Sepúlveda, P. (1991) Hoja Illapel- Región de Coquimbo. Serv. Nac. Geol. y Min., Chile. Carta Geológica N° 69, 132p.

Roser, B. and Korsch, R. (1986) Determination of tectonic setting of sandstone-musdstone suites using SiO_2 content and K_2O/Na_2O ratio. J. Geol., v. 94, pp. 635-650.

Roser, B. and Korsch, R. (1988). Provenance signatures of sandstones-mudstone suites determined using discriminant function analysis of mayor-element data. Chem. Geol., v. 67, pp. 119-139.

Rubinstein, N., Bevins, R., Robinson, D.and Morello, O. (1998) Very low grade metamorphism in the Alcaparrosa Formation, Western Precordillera, Argentina. 10° Congr. Latinameric. Geol. and 6° Congr. Nac. Geol. Económica, Actas, 2, pp. 226-229.

Ruviños, M., Gregori, D. and Bjerg, E. (1997) Condiciones de P y T del basamento metamórfico de la Cordillera Frontal de Mendoza. 8° Congr. Geol. Chileno, Actas, 2, pp. 1512-1516.

Stappenbeck, R. (1917) Geología de la falda oriental de la Cordillera del Plata. Min. Agric. Nación. Secc. Geol., Mineral. y Minería, Buenos Aires. Anales 10, pp. 1-49.

Sun, S. (1982) Chemical composition and origin of the earth's primitive mantle. Geochim. Cosmochim. Acta, v. 46, pp. 179-192.

Sun, S. and McDonought, W. (1989) Chemical and isotopic systematics of oceanic basalts: implications for mantle composition and processes. In: Saunders, A. and Norry, M. (Eds.), Magmatism in ocean basins. Geol. Soc., London, Spec. Pub., v. 42, pp. 313-345.

Taylor, S. and McLennan, S. (1985) The continental crust: its Composition and evolution. Blackwell Scientific, Oxford, 312p.

Totten, M.W., Hanan, M.A. and Weaver, B.L. (2000) Beyond whole-rock geochemistry of shales: The importance of assessing mineralogical controls for revealing tectonic discriminates of multiple sediments sources for the Ouachita Mountain flysh deposits. Geol. Soc. Amer., Bull., v. 112, pp. 1012-1022.

Turner, F.J. and Verhoogen, J. (1975) Petrología ígnea y metamórfica. Omega, Barcelona, 726p.

Vujovich, G.I. and Gregori, D. (2001) Cordón del Portillo, Cordillera Frontal, Mendoza: Caracterización geoquímica de las metamorfitas. 15° Congr. Geol. Argentino, Actas 1, pp. 217-222.

Wood, D. (1980) The application of the Th-Hf-Ta diagram to problems of tectonomagmatic classification to establishing the nature of the crustal contamination of basaltic lavas of the British Tertiary volcanic province. Earth Planet. Sci. Lett., v. 50, pp. 11-30.

Zardini, R.A. (1962) Significado geológico de las serpentinitas de Mendoza. Anales Primeras J. Geol. Argentinas, v. 2, pp. 437-442.